Bioelectrochemistry and Bioenergetics 4, 447–463 (1977)

Adsorption of Adenine at an Aqueous Solution|Mercury Interface *

by MARK A. JENSEN, TIMOTHY E. CUMMINGS and PHILIP J. ELVING

The University of Michigan, Ann Arbor, Michigan, 48109, U.S.A.

Manuscript received May 28th 1977

Summary

The faradaic and non–faradaic capacitive currents and other behavioral manifestations seen for a 10 μM solution of adenine in pH 4.8 MCILVAINE buffer (0.5 M ionic strength) on *d.c.* polarography, phase–selective *a.c.* polarography, normal pulse polarography, and rapid scan–rate cyclic voltammetry (including linear potential sweep amperometry) at dropping mercury and hanging mercury drop electrodes, have been analyzed in terms of the adsorptive behavior of the adenine and of chemical reactions coupled to the adsorption of adenine and its faradaic reduction in the adsorbed and unadsorbed states. Important variables included the prepolarization potential, *i.e.*, the potential at which the electrode was held prior to initiation of a perturbation in terms of an increase in potential, and the periods of time for which the prepolarization potential was maintained and during which the potential perturbation occurred, as well as the period of time before the current was sampled after the perturbation was applied.

Introduction

The study of the nucleic acid bases, adenine and cytosine, and their derivatives by polarographically based and other electrochemical techniques has always indicated the importance of the adsorption of the nucleic acid derived species at the solution|electrode interface, especially at mercury electrodes (*e.g.*, Refs. 1 to 4). The increasing interest in recent years in examining by electrochemical means the adsorptive and faradaic behavior of complex natural and biosynthetic polynucleotides extending up to DNA itself (*e.g.*, Refs. 5 to 9), has generated a number of recent studies on the adsorptive behavior of simpler adenine derivatives, *e.g.*,

* Discussed at the Symposium on "Biopolymers in Adsorbed State", held at Weimar (G.D.R.), 26–28 April 1977.

those of KRZNARIC, VALENTA and NÜRNBERG[10] on the adenine mononucleotides and of FLEMMING[11] on adenine itself.

FLEMMING's study[11] utilized normal pulse polarography of 6 μM adenine in pH 5 MCILVAINE buffer giving particular attention to the effect of adsorption of adenine during the prepolarization period on the faradaic wave height observed. The present study is supplementary to FLEMMING's in that 10 μM adenine in pH 4.8 MCILVAINE buffer of 0.5 M ionic strength was examined by normal pulse polarography, *d.c.* D.M.E. polarography, phase–selective *a.c.* polarography, and cyclic voltammetry, which, in effect, included linear potential sweep amperometry, with particular reference to the information, which these techniques would yield, with respect to the adsorption of adenine.

The general mode of experimentation in the pulse and cyclic studies was to hold the potential of the electrode (prepolarization potential, U_{pp}) constant for a given period of time (prepolarization time, t_{pp}) and then to examine the faradaic and capacitive currents produced on potential variation. U_{pp} and t_{pp} were varied over normally significant ranges. In order to remove certain possible artifacts and ambiguities, the current data were in many instances normalized as current density data derived from the apparent real electrode area, *e.g.*, the usually computed spherical electrode area corrected for the capillary orifice area and possible shielding.

The ranges of agreement and disagreement, indicated in respect to the adsorption of adenine by the various techniques, were examined in order to see if the differences were explicable in terms of the inherent characteristics of the different techniques, as well as in regard to the additional information which might be obtained about the behavior of adenine.

Experimental

Chemicals

MCILVAINE buffer (pH 4.8; 0.5 M ionic strength) was prepared from reagent grade chemicals.[12] The 10 μM adenine (NATIONAL BIOCHEMICALS CORP.) solution was prepared by dilution of 1.0 mM adenine solution by the pH 4.8 buffer. Mercury for electrodes was chemically purified and distilled. Water was suitably distilled.

Instrumentation

All data were obtained using a jacketed electrochemical cell thermostatted at 25 °C. A LUGGIN capillary was positioned within 1 to 2 drop–diameters of the hanging mercury drop electrode (H.M.D.E.), or 3 to 4 mm of the dropping mercury electrode (D.M.E.) drop. The H.M.D.E. was a platinum contact–type electrode; the Hg drop consisted of two

drops collected from the D.M.E. The D.M.E. was set to give a mean Hg flow-rate at open-circuit of 0.98 mg/s for *a.c.* polarography and 1.10 mg/s for pulse polarography. Natural drop-times were used for the *d.c.* polarographic diffusion control study ; for all other work, the D.M.E. drop-knocker was activated by synchronization timing circuitry in the potentiostat.

The potentiostat was built in-house and was designed for very high speed electrochemical kinetic studies. The TELEDYNE PHILBRICK Model 1025 operational amplifiers employed have a maximum voltage range of ± 10 V, a maximum current range of ± 50 mA, and an open loop slewing rate of 5×10^8 V/s. The sample-and-hold amplifier (Hybrid Systems Model 725 LH) has a maximum output voltage of ± 10 V, a data acquisition time of 10 μs for 0.01 % tracking of a 10-V change in signal, and an output droop specified as 15 mV/s (the unit used shows an output droop of 0.25 mV/s).

A HEWLETT-PACKARD Model 3440A digital voltmeter was used to monitor the applied *d.c.* potentials.

For *a.c.* polarography, a PRINCETON APPLIED RESEARCH Model 121 lock-in amplifier was used both as a source for the applied 10 mV p-p *a.c.* modulation signal and as a phase-selective detector of the *a.c.* signal from the potentiostat's current amplifier.

WAVETEK Model 112 and 114 function generators were used to generate triggerable, variable-period, square-wave pulses, and the triangular waveform.

A HEWLETT-PACKARD Model 7005 X-Y recorder was generally used for data display. For observation of transient signals and for rapid-scan cyclic voltammetric data acquisition, a TEKTRONIX Model 5103N oscilloscope with Type 5A15N and 5A18N voltage-amplifier plug-ins and Type 5B10N time-base was used.

Procedures

Solutions were deaerated with water-pumped nitrogen for 30 min before data acquisition. The nitrogen was passed through two gas towers containing V(II) solution in HCl over amalgamated zinc to remove residual oxygen, a $Ca(OH)_2$ tower to remove entrained HCl, and, finally, a distilled H_2O tower to water-saturate the N_2. A nitrogen atmosphere was maintained in the electrochemical cell during experiments by continuously passing N_2 over the cell solution.

d.c. polarographic data were obtained at a potential scan rate of 2 mV/s.

a.c. polarographic data acquisition required careful adjustment of the *a.c.* modulation amplitude, and the lock-in amplifier phase-angle and frequency trim adjustments. Because phase-angle measurements are relative to the potential applied to the working electrode, all lock-in amplifier detector adjustments were made using the output of the potentiostat's voltage follower as the input signal, thereby correcting for any phase shifts due to the controller amplifier. The frequency trim of

the lock–in was adjusted to maximize the detector output response in the in–phase mode; then, the detector was switched to the out–of–phase (quadrature) mode and the phase angle was adjusted to give a null signal. These two steps insured that the lock–in amplifier was tuned to the frequency of the applied *a.c.* modulation voltage and that this latter voltage was defined as the 0° reference angle signal. Since a 10–mV p–p *a.c.* modulation voltage was used, the lock–in gain was adjusted to give a full–scale response to the voltage follower output at the 10–mV full–scale sensitivity. This last step serves as an internal correction for any error in setting the amplitude of the modulation voltage.

For data acquisition, the output of the lock–in was monitored by the sample–and–hold amplifier. To filter out spurious noise during the sampling period, a 300–ms time constant was used on the lock–in output. The applied *d.c.* voltage was scanned at 5 mV/s when 2 s drop–times were used and at 2 mV/s for 5 s drop–times.

Cyclic voltammetry was performed on both the H.M.D.E. and the D.M.E., using the WAVETEK 112 signal generator as a source of triangular wave forms. A new Hg drop was used for each cyclic voltammogram.

Normal pulse polarography involved the following adaptation of the potentiostat's timing circuitry. Pulse application was effected using the triggered mode, square–wave output of the WAVETEK 112; the frequency was set to give a 3.0–ms pulse duration. Pulse application was synchronized to the drop–knocker using one of the potentiostat's internal synchronization pulses to trigger the WAVETEK 114 which served as a timing delay to trigger the WAVETEK 112. Adjustment of the WAVETEK 114 frequency permitted synchronization so that the 3.0–ms pulse application occurred at the end of the drop–life. To insure that the pulse did not terminate while the sample–and–hold amplifier was either sampling or transitting from the sample mode to the hold mode, the delay was set so that the pulse terminated 0.05 to 0.1 ms after sampling ceased; thus, the pulse was applied during the last 2.95 ± 0.05 ms of the drop–life. Because the sample–and–hold amplifier data–acquisition time is only 10 μs, the time after application of the pulse and before data acquisition (the discharge time) is 2.94 ± 0.05 ms.

All potentials are referred to the aqueous saturated calomel electrode.

Data analysis

Electrode area determination

Determination of current densities, j, for pulse polarographic measurements and of differential capacitance, C_{dl}, from *a.c.* polarographic data, requires knowledge of the electrode area. PERRAM, *et al.*,[13] showed that assuming the drop to be spherical results in calculated areas generally within 0.5 % of that calculated for a pendant drop shape. MOHILNER, *et al.*,[14] emphasized the importance of correcting for the contact area

between the Hg drop and the Hg ribbon at the D.M.E. capillary orifice; computer controlled data acquisition allowed a large number of drop–times to be measured at each potential, which permitted a data analysis procedure that is not amenable to the finite amount of data acquired without computer control. The procedure used in the present study is based on equations (6) and (7) of Ref. 14, since the *a.c.* capacitance current can be easily related to the bridge–measured capacitance and the *a.c.* capacitance current density can be related to the differential capacitance.

The effective electrode area, A_t, is related to the calculated spherical drop area, A_s, by equations (1) and (2), where A_0 includes the contact area with the capillary orifice and any shielding effects of the glass capillary, m is the flow rate of mercury, ρ is the density of mercury, and t_1 is the drop–time.

$$A_t = A_s - A_0 \tag{1}$$

$$A_s = \left(\frac{6\sqrt{\pi}\, m}{\rho}\right)^{2/3} \tag{2}$$

The measured *a.c.* capacitance current, $I_{a.c.}$, equals the product of the *a.c.* capacitance current density, $j_{a.c.}$, and the effective electrode area; substitution of equations (1) and (2) for A_t leads to equation (3).

$$I_{a.c.} = j_{a.c.}\left(\frac{6\sqrt{\pi}\, m}{\rho}\right)^{2/3} t_1^{2/3} - j_{ac}A_0 \tag{3}$$

Eq. 3 suggests that, if $I_{a.c.}$ is measured at various drop–times, a plot of $I_{a.c.}$ *vs.* $t_1^{2/3}$ should be linear with an intercept equal to $-j_{a.c.}A_0$ and an intercept to slope ratio of $-A_0/(6\sqrt{\pi}\, m/\rho)^{2/3}$, from which A_0 can be evaluated once m is determined.

Numerical correction for uncompensated resistance

In the case of *a.c.* polarography, the *a.c.* capacitance current is 90° out of phase with the *a.c.* modulation voltage at the working electrode, ΔU_w. (The phase relationships are shown in Fig. 1). Because the 0° reference signal is defined as the output of the voltage follower, any phase shift through the LUGGIN capillary–reference electrode–voltage follower network and/or any uncompensated resistance in solution between the tip of the LUGGIN capillary and the working electrode, R_u, will result in a non–zero phase angle between the *a.c.* signal at the voltage follower output, ΔV, and the *a.c.* modulation voltage at the working electrode. In addition, an uncompensated resistance will result in an $I_{a.c.}R_u$ loss, which decreases ΔU_w below ΔV.

Because the differential capacitance is given by equation (4,) where f is the *a.c.* frequency in Hz, it is necessary to evaluate ΔU_w.

$$C_{dl} = \frac{I_{a.c.}}{2\pi f \Delta U_w A_t} \tag{4}$$

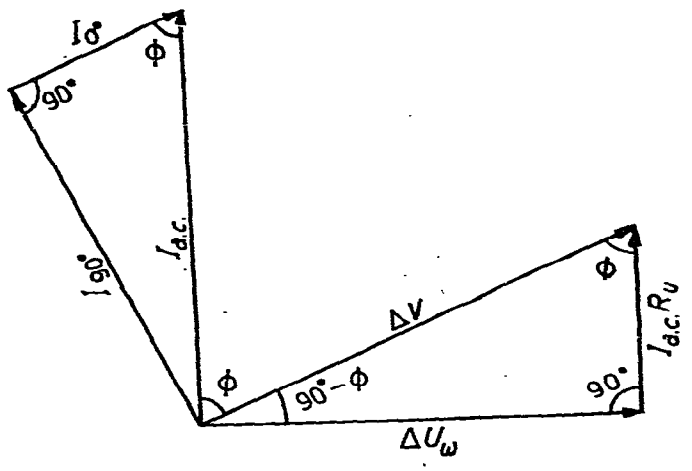

Fig. 1.
Phase relationships encountered in *a.c.* poarlography. Symbols are defined in the text.

In the presence of a non–zero R_u, $I_{a.c.}$ has a phase angle, Φ, relative to the 0° degree reference signal, ΔV, which is *not* 90°; hence, it is necessary to record both the inphase and quadrature modes of the current amplifier output. The value of $I_{a.c.}$ is then obtained using equation (5).

$$I_{a.c.} = \sqrt{I_{0°}^2 + I_{90°}^2} \tag{5}$$

The phase angle, Ø, at any applied value of $U_{d.c.}$ is given by

$$\Phi = \arctan \frac{I_{90°}}{I_{0°}} \tag{6}$$

The uncompensated resistance and ΔU_w can be evaluated from equations (7) and (8), respectively.

$$R_u = \frac{\Delta V}{I_{a.c.}} \cos -\Phi \tag{7}$$

$$\Delta U_w = \Delta V \sin -\Phi \tag{8}$$

Results

D.M.E. contact area. a.c. polarographic in–phase and quadrature currents for the McIlvaine buffer alone were measured at 400 Hz and $U_{d.c.} = -0.24$ V for drop–times of 2 s, 3 s, and 5 s. The value of $I_{a.c.}$ at each t_1 was determined by equation (5); ΔU_w was evaluated at each t_1, using equation (8). The measured $I_{a.c.}$ values were corrected for variations in ΔU_w by means of equation (9).

$$I_{a.c.} = I_{a.c.}\ (\text{measured}) \frac{\Delta V}{\Delta U_w} \tag{9}$$

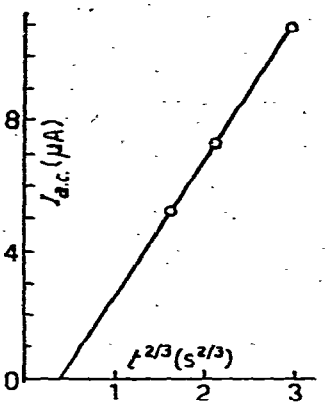

Fig. 2.

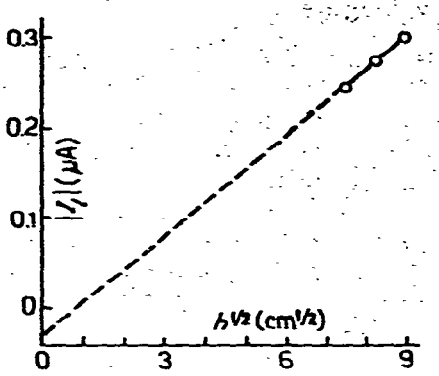

Fig. 3.

Fig. 2.
Plot of *a.c.* polarographic data for determination of the effective contact area of the D.M.E. with the capillary orifice, using equation 3.

Fig. 3.
Variation of D.M.E. *d.c.* polarographic limiting current (background-corrected) for 10 μ*M* adenine in pH 4.8 McIlvaine buffer with mercury height (corrected for back pressure).

In the subsequent discussion, tables and figures, the $I_{a.c.}$ cited and its magnitudes are always those corrected for resistance by means of equation (9), unless otherwise specified. A plot of $I_{a.c.}$ *vs.* $t_1^{2/3}$ (Fig. 2) yielded a slope of 4.340 μA $s^{-2/3}$ and an intercept of —1.705 μA, from which A_0 was calculated to be 0.0033 cm^2 based on $m = 0.98$ mg/s.

d.c. polarography. Because the presence of adenine shifted the background discharge potential *ca.* 0.05 V more positive with the adenine wave appearing on the rising portion of background discharge, direct subtraction of the background current was not possible. On shifting the background polarogram 0.05 V positive, the difference in current between adenine solution and background showed a polarographic wave with a level plateau. Data at two different column heights are given in Table 1; a plot of I_l *vs.* $h^{1/2}$ is a straight line (Fig. 3).

Normal pulse polarography. Normal pulse polarographic currents and current densities obtained by stepping from the prepolarization potential, U_{pp}, to —1.48 V after prepolarization times, t_{pp}, of 2 s or 5 s, are shown in Fig. 4 and 5. For background solutions containing only the buffer, the charging current due to the pulse was observed to decay to a magnitude of 1 to 2 μA within 0.2 ms.

a.c. polarography. Differential capacitance values for the background solution before and after addition of 10 μ*M* adenine are given in Tables 2 and 3, and Fig. 6. The change in the differential capacitance, ΔC_{dl}, due to the presence of adenine is shown in Fig. 7.

Table 1. *d.c.* polarographic behavior at the D.M.E. of adenine as a function of mercury height[a].

h (cm)	55.5	80.5
m (mg/s)	1.27	1.86
t_1 (s)	5.15	3.56
I_l (μA)	0.244	0.300
I_d	13.5	13.8
$U_{½}$ (V)	—1.365	—1.370

[a] Conditions: 10 μM adenine in pH 4.8 McIlvaine buffer (ionic strength = 0.5 M) at 25 °C; scan rate, v = 1.9 mV/s. The mercury height, h, is corrected for back-pressure. The limiting current, I_l, is corrected for the current shown by the background electrolyte solution alone. Units for the diffusion current constant, I_d, are μA $s^{1/2}$/mM $mg^{2/3}$.

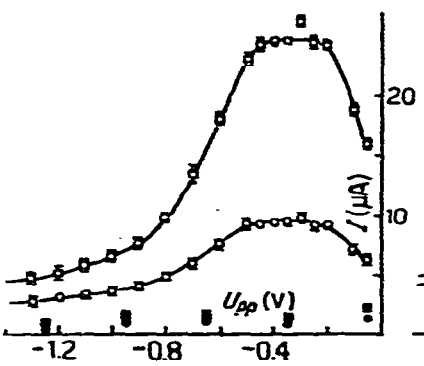

Fig. 4.

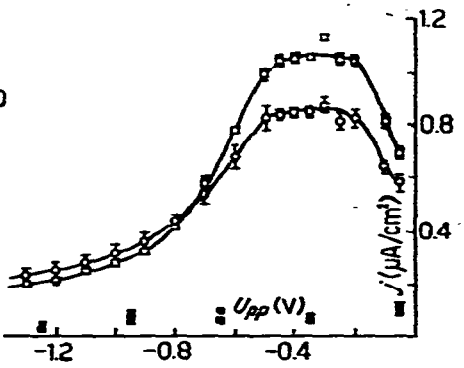

Fig. 5.

Fig. 4.
Currents obtained for 10 μM adenine in pH 4.8 McIlvaine buffer on normal pulse polarography on stepping the potential from the prepolarization potential shown to —1.48 V after prepolarization times of 2 s (circles) and 5 s (squares); the bottom two curves are for the buffer alone. The discharge period was 3 ms; the current measurement period was 10 μs.

Fig. 5.
Current densities obtained for 10 μM adenine in pH 4.8 McIlvaine buffer on normal pulse polarography on stepping the potential from the prepolarization potential shown to —1.48 V after prepolarization times of 2 s (circles) and 5 s (squares); the bottom two curves are for the buffer alone. The discharge period was 3 ms; the current measurement period was 10 μs.

Cyclic voltammetry. Initial investigations using a platinum–contact H.M.D.E. showed behavior inconsistent with the results from pulse and *a.c.* polarography. Cathodic–anodic peak pairs centered at about —1.05 V and —1.27 V were observed, whose irreproducible behavior, coupled with the absence of any indication for faradaic activity at —1.05 V by *a.c.*, *d.c.* or pulse polarography, suggested that the presence of platinum in the H.M.D.E. might be causing the odd behavior. Cyclic voltammetry at a D.M.E. with a drop–time of 14 s at —0.45 V showed a cathodic peak (U_p of about —1.5 V); no other peaks were observed, except for a cathodic peak (U_p = —0.74 V), which appeared only when U_{pp} was positive of —0.45 V. Use of the platinum–contact H.M.D.E. was abandoned and all cyclic data were obtained at a D.M.E. with a natural drop–time of 14 s.

Table 2. Double–layer capacitance of pH 4.8 McIlvaine buffer (μ = 0.5 *M*) as a function of potential, frequency[a], and drop–time.

$-U_{dc}$ (V)	C_{dl} (μF/cm^2)		
	160 Hz		1,000 Hz
	t_1 = 5 s	t_1 = 2 s	t_1 = 2 s
0.050	—	—	30.40[c]
0.100	—	23.87[b]	24.53
0.150	22.19[b]	21.68	21.86
0.200	21.16	20.79	20.72
0.250	20.65	20.29	20.31
0.300	20.17	19.89	19.94
0.350	19.47	19.30	19.40
0.400	18.53	18.40	18.41
0.450	17.27	17.21	17.35
0.500	16.05	15.92	16.00
0.550	14.55	14.52	14.51
0.600	13.18	13.13	13.08
0.700	10.98	10.84	10.77
0.800	9.57	9.47	9.33
0.900	8.73	8.63	8.50
1.000	8.40	8.33	8.26
1.100	8.35	8.26	8.09
1.200	8.44	8.31	8.21
1.300	8.73	8.55	8.53

[a] ΔU_w = 10 mV p–p.

[b] The estimated uncertainty in the data in this column is ±0.05 μF/cm^2.

[c] The estimated uncertainty in the data in this column is ±0.08 μF/cm^2.

Table 3. Double-layer capacitance of adenine as a function of potential, frequency, and drop-time[a].

$-U_{dc}$ (V)	C_{dl} (μF/cm²)		
	160 Hz		1,000 Hz
	$t_1 = 5$ s	$t_1 = 2$ s	$t_1 = 2$ s
0.050	—	—	30.82[c]
0.100	—	24.07[b]	24.56
0.150	21.87[b]	21.68	21.71
0.200	20.46	20.49	20.50
0.250	19.75	19.89	19.78
0.300	19.24	19.40	19.31
0.350	18.53	18.70	18.65
0.400	17.60	17.71	17.73
0.450	16.23	16.51	16.62
0.500	15.16	15.32	15.37
0.550	13.98	14.13	14.12
0.600	12.72	12.93	12.89
0.700	10.79	10.84	10.82
0.800	9.57	9.25	9.47
0.900	8.72	8.75	8.64
1.000	8.30	8.16	8.28
1.100	8.30	8.16	8.16
1.200	8.54	8.16	8.28
1.300	8.82	8.55	8.55

[a] Conditions: 10 μ*M* adenine in pH 4.8 McIlvaine buffer ($\mu = 0.5$ *M*) at 25 °C; $\Delta U_w = 10$ mV p-p.

[b] The estimated uncertainty in the data in this column is ±0.05 μF/cm².

[c] The estimated uncertainty in the data in this column is ±0.08 μF/cm².

Using a sweep or scan rate, v, of 316 V/s and beginning the sweep 12 s after the drop-birth, the variation of peak current for the peak at —1.5 V was investigated as a function of U_{pp}. Since the time after drop-birth, at which the cyclic scan is initiated, is the prepolarization time, it will be referred to as t_{pp}. The dependence of $I_p/Acv^{1/2}$ on U_{pp} is shown in Fig. 8.

The scan-rate dependence of I_p is shown in Fig. 9 and 10; v was varied from 104 to 633 V/s. Slower scan rates could not be employed because the low concentration of adenine (10 μ*M*) yielded currents with too low a signal-to-noise ratio for meaningful evaluation.

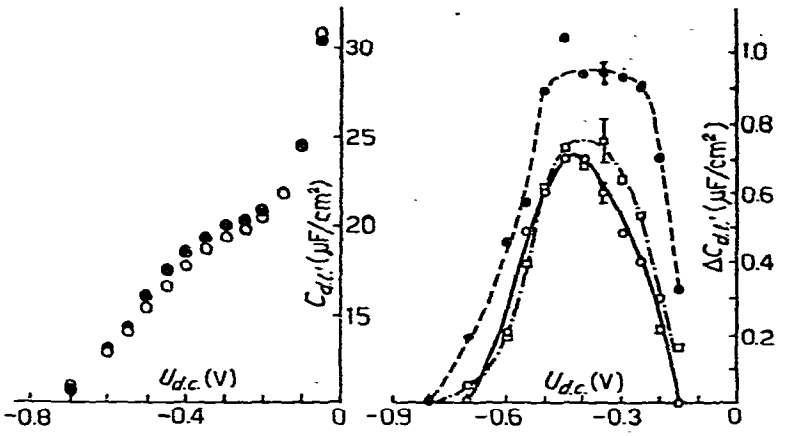

Fig. 6. Fig. 7.

Fig. 6.
Double-layer capacitance for pH 4.8 McIlvaine buffer alone (●) and after the addition of 10 μM adenine (○). Conditions: 10 mV p-p at 1,000 Hz; 2 s drop-time.

Fig. 7.
Double-layer capacitance change on addition of 10 μM adenineto pH 4.8 McIlvaine buffer ($\mu = 0.5$ M). ○: 160 Hz and 2 s drop-time; ●: 160 Hz and 5 s drop-time; □: 1,000Hz at 2 s drop-time.

Variation of t_{pp} was used to determine whether the adsorption of adenine was sufficiently rapid to achieve equilibrium within a few seconds. The relation of the I_p function to t_{pp} for two prepolarization potentials is shown in Fig. 11.

Discussion

a.c. polarography

The standard electrochemical method for determining the extent of adsorption at an electrode|solution interface is measurement of C_{dl} as a function of applied potential and of bulk adsorbate concentration. Elaborate data analysis procedures[15] permit evaluation of the surface excess of adsorbed species from such data. With simple data analysis techniques, the surface excess cannot be determined, but qualitative information with regard to the extent of adsorption as a function of potential and concentration is obtained. Since the magnitude of C_{dl} is dependent on the extent of adsorption, the difference between C_{dl} for the background and adsorbate-containing solutions, ΔC_{dl}, is a measure of the extent of adsorption.

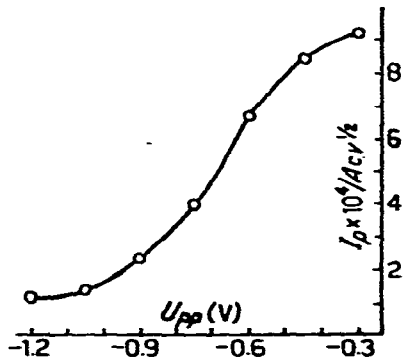

Fig. 8.
Variation of cyclic voltammetric peak current function for 10 μM adenine in pH 4.8 McIlvaine buffer with prepolarization potential. Scan rate = 316 V/s. Prepolarization time = 12 s. (The ordinate must read $I_p \times 10^{-4}/ACV^{1/2}$).

Because measurements of C_{dl} do not rely on faradaic activity of the adsorbate, data interpretation is simplified. When a faradaic process is used to monitor the extent of adsorption, problems arise regarding the mechanism of the faradaic discharge, *i.e.*, the concentration–dependence of the I–c relationship, the extent to which non–adsorbed diffusing species contribute to the measured faradaic current, and the associated matter of the diffusion gradient profile produced by the adsorption process if equilibrium coverage has not been achieved and the diffusion gradient destroyed before the onset of faradaic activity (the latter problem is always present at the D.M.E. to a greater or lesser extent because of the changing electrode area).

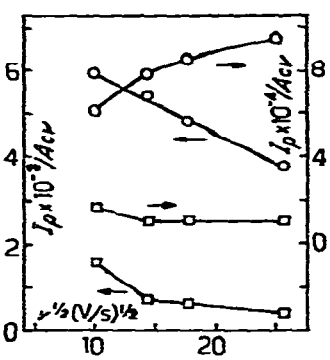

Fig. 9.

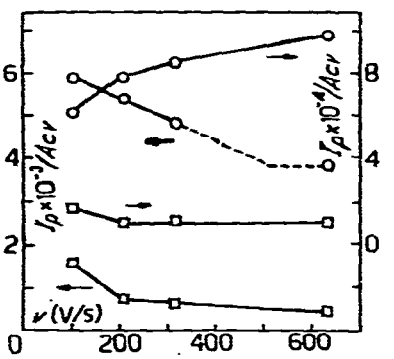

Fig. 10.

Fig. 9
Variation of cyclic voltammetric peak current functions for 10 μM adenine in pH 4.8 McIlvaine buffer with square root of scan rate for prepolarization potentials of —0.45 V (○)and —1.20 V (□), and a prepolarization time of 12 s.

Fig. 10.
Variation of cyclic voltammetric peak current functions for 10 μM adenine in pH 4.8 McIlvaine buffer with scan rate for prepolarization potentials of —0.45 V (○) and —1.20 V (□), and a prepolarization time of 12 s.

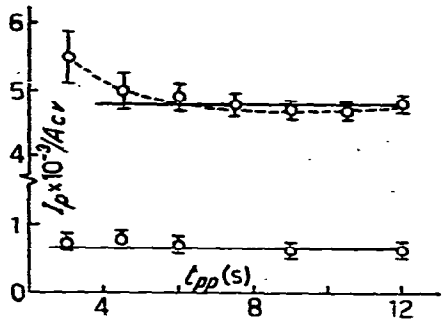

Fig. 11.
Variation of cyclic voltammetric peak current function for 10 μM adenine in pH 4.8 McIlvaine buffer with prepolarization time for prepolarization potentials of —0.45 V (upper plot) and — 1.20 (lower plot) scan rate = 316 V/s.

Because the relative surface excess of adsorbate is independent of electrode area in the absence of kinetically controlled processes, *e.g.*, the McIlvaine buffer solution without adenine, the values of C_{dl} determined at two different electrode areas should agree, provided the correct electrode area magnitudes are used in equation (4) to evaluate C_{dl}. This fact provides a means for testing the validity of the orifice area correction. The excellent agreement between C_{dl} measured at $t_1 = 2$ and 5 s at 160 Hz for the buffer solution alone (Table 2) supports the correction's being valid. Additionally, the agreement between the data at 160 and 1000 Hz (Table 2) and the fact that A_0 was evaluated at 400 Hz indicate that A_0 is frequency-independent. Over the range of —0.150 to —1.300 V, the mean difference between C_{dl} measured at $t_1 = 2$ and 5 s at 160 Hz is 0.17 μF/cm^2 (standard deviation = 0.13 μF/cm^2). Although the values at $t_1 = 2$ s are always lawer than those at $t_1 = 5$s the mean difference is only 1 to 2 % of the C_{dl} values, which is within the combined experimental uncertainties of the instrumentation, the mechanical measurement of recorded data, and the precision to which the electrode areas are known ; however, the facts that the mean difference between C_{dl} measured at 160 and 1000 Hz at $t_1 = 2$ s is only 0.08 μF/cm^2 (standard deviation = 0.05 μF/cm^2) and that the differences are not systematic, suggest the main source of error between the data at 2 and 5 s to be the values of A_t.

In the case of the adenine solution at 160 Hz (Table 3), C_{dl} for $t_1 = 5$ s are systematically lower than at $t_1 = 2$ s over the range of —0.200 to —0.700 V, which is exactly opposite to the situation for the buffer alone. At potentials more negative than —0.7 V, where adenine is apparently not significantly adsorbed, C_{dl} at $t_1 = 5$ s are again generally larger than at $t_1 = 2$ s, as for the buffer alone. Thus, it would appear that the lower C_{dl} at 5 s as compared to those at 2 s are due to the presence of adenine and not to an error in the A_t values ; in fact, the results for the buffer alone suggest that, were more precise values of A_t available, an even larger difference between C_{dl} at 2 s and 5 s might be observed for adenine over the potential region in which adsorption occurs. Consequently, the significant increase in ΔC_{dl} at —0.2 to —0.5 V for $t_1 = 5$ s over the corresponding values at $t_1 = 2$ s suggests that a slow kinetic

process may be associated with the adsorption of adenine. The nature of the kinetic process may be surmised from the following considerations.

At 2 s drop–time, the adenine adsorption appears to reach a maximum at —0.40 to —0.45 V (Fig. 7); at 5 s, the adenine adsorption appears to be constant over a wide potential interval. The ratio of the maximum change in C_{dl} at 5 s to that at 2 s for 160 Hz is 1.21, whereas the corresponding ratio for data at 5 s and 160 Hz to data at 2 s and 1000 Hz is 1.16. The region of maximum adsorption is positive of the potential of zero charge; since *ca.* 15 to 20 % of the adenine is protonated at pH 4.8 and, therefore, positively charged, coulombic repulsion between electrode surface and protonated adenine will occur. Kinetically controlled steps may be involved in the equilibrium between protonated and unprotonated adenine on the electrode surface and in solution.

Although the *a.c.* polarographic data indicate some deviation of the adenine solution capacitance from background solution capacitance at potentials negative of —0.8 V (Tables 2 and 3), a very low frequency noise problem (*ca.* 0.008 Hz) resulted in most ΔC_{dl} values measured at these more negative potentials being within the estimated measurement uncertainty for a zero difference, as well as being considerably smaller than the peak–to–peak amplitude of the low frequency noise.

Normal pulse polarography

The pulse polarographic results show a trend similar to the ΔC_{dl} behavior shown by *a.c.* polarography; however, the pulse data at $t_1 = 2$ s show a much broader maximum (about —0.2 V to —0.5 V) than do the differential capacitance results.

The ratio of the current density, j, (corrected for capillary orifice) in the region of maximum adsorption for $t_{pp} = 5$ s to that for $t_{pp} = 2$ s is 1.24, which is close to the 1.21 for the corresponding ΔC_{dl} ratio at 160 Hz (cf. previous section). It must be made clear that the parameters being considered, ΔC_{dl} and j, have — by definition — been corrected for a change in electrode area. The pulse polarographic currents, I, at the region of maximum adsorption show a $(t_{pp})^{0.9}$ dependency.

Since the drop area is changing more rapidly at $t = 2$ s than at $t = 5$ s (the natural drop–time was *ca.* 5.8 s), the rate of adsorption of adenine at 2 s should be larger than at 5 s; hence, a steeper concentration gradient will be present for $t_{pp} = 2$ s with the contribution by diffusing species to the total faradaic current being smaller than at $t_{pp} = 5$ s. Because the equilibrium surface excess of adsorbate is related to the surface concentration of non–adsorbed species, the presence of a diffusion gradient, which decreases the latter, will also lower the relative surface excess of adsorbate; consequently, the relative surface excess at $t = 2$ s will be lower than at $t = 5$ s, provided saturation surface coverage is not achieved.

As U_{pp} becomes very negative, the ratio of j at $t_{pp} = 2$ s and 5 s increases and seems to reach a limiting value of 1.15 to 1.16 at $U_{pp} =$ —1.3 V. As subsequently discussed, (cf. sections on *d.c.* polarography

and cyclic voltammetry), the faradaic wave with $U_{1/2} = -1.37$ V may involve catalytic hydrogen discharge. From I–t curves at the D.M.E. for catalytic discharges by low molecular weight substances, STACKELBERG and FASSBENDER[16] found that the current was proportional to t^k, where $k = 0.5$ to 0.6 ; the current at any instant in the drop–life was independent of the stage in the drop–life at which the discharge voltage was applied. Thus, a k of 0.5 would predict a $(t_{pp})^{-1/6}$ relationship for j, as is observed at very negative potentials.

d.c. polarography

The relationship between the limiting current of the cathodic adenine wave, I_l, and corrected mercury column height, h, (Fig. 3) indicates that I_l is diffusion–controlled. The small non–zero intercept is probably due to the considerable distance over which the straight line fit must be extrapolated to $h^{1/2} = 0$; in fact, within the uncertainty of the experimental results[33], a straight line with a zero intercept may be fitted to the data. The large I_d values (Table 1), which indicate an unlikely six– to seven–electron transfer, are most likely due to hydrogen discharge catalyzed by adenine or a reduction product superimposed on the adenine reduction. Catalytic discharge would not be surprising, since the wave appears at the onset of background discharge, which is itself shifted positive by the presence of adenine and its reduction product.[2,17] Because the wave appears to be diffusion–controlled, the rate of hydrogen discharge must be dependent upon a diffusing species, *i.e.*, adenine.

Cyclic voltammetry

The cyclic voltammetric peak current function results (Fig. 8 to 11) indicate a trend for adenine adsorption as a function of U_{pp} (Fig. 8), which is similar to those suggested by *a.c.* and normal pulse polarography. The large values of $I_p/Acv^{1/2}$ at very negative U_{pp}, *e.g.*, —1.2 V, where adenine is apparently desorbed, again suggest that catalytic hydrogen discharge occurs. The behavior of the function $I_p/Acv^{1/2}$ at $U_{pp} = -1.2$ V with increasing scan rate (Fig. 9 and 10) indicates that a kinetically controlled process is being outrun at 200 V/s. This process may be the formation of reducible, protonated adenine at the interface since faradaic consumption of the protonated species shifts the equilibrium between the unprotonated and protonated adenine.

The two functions, $I_p/Acv^{1/2}$ and I_p/Acv, for $U_{pp} = -0.45$ V show opposite trends (Fig. 9 and 10). Because adsorption occurs at —0.45 V, there should be a large concentration of adenine near the electrode surface ; however, if the scan from U_{pp} to U_p were sufficiently rapid that diffusion of the desorbed adenine were negligible once the applied potential was such that desorption occurred, then :

(1) a plot of $I_p/Acv^{1/2}$ *vs.* $v^{1/2}$ should be linear with a positive slope equal to I_p/Acv. Fig. 9 suggests that, at v of 316 V/s or larger, the

$I_p/Acv^{1/2}$ *vs.* $v^{1/2}$ relation becomes linear ; however, the slope is only 1.6×10^3 compared to an expected 3.8×10^3 or greater ;

(2) a plot of I_p/Acv *vs.* v should be independent of scan rate ; Fig. 10 suggests that this is so for $v >$ ca. 500 V/s. The facts that I_p/Acv decreases with increasing v and $I_p/Acv^{1/2}$ *vs.* $v^{1/2}$ does not show as large a slope as expected, suggest that none of the adenine, which desorbs during the scan, is lost by diffusion, but that, at faster scan rates, some preceding chemical reaction, *e.g.*, protonation of adenine, is being outrun, or that the following steps in an E.C.E. mechanism, *e.g.*, catalytic hydrogen discharge, are being outrun. Since $I_p/Acv^{1/2}$ for $U_{pp} = -1.2$ V (Fig. 9) appears to become constant, catalytic hydrogen discharge may not be outrun.

The information presented in the preceding paragraph suggests the following :

(1) none of the adenine, which desorbs during the scan, diffuses away from the electrode ;

(2) if the value of I_p/Acv at 633 V/s is assumed to be due solely to the equilibrium concentration of adsorbed, protonated adenine, and the surface concentration of non-adsorbed adenine is assumed to be small, then, by extrapolating the I_p/Acv *vs.* v data to $v = 0$, the relative amounts of protonated and unprotonated adenine adsorbed can be obtained. Extrapolation provides an intercept value for I_p/Acv of 6.45×10^3. For a limiting value at $v = 633$ V/s of 3.8×10^3, which is due solely to adsorbed protonated adenine, 59 % of the adsorbed adenine would be in the protonated form at pH 4.8. If the bulk solution proton activity, 1.6×10^{-5} M, is used as the proton activity term, a pK_a of 5.0 is obtained for adsorbed adenine at $U_{pp} = -0.45$ V. Due to coulombic interaction between the electrode and the protonated adenine, pK_a is expected to be potential-dependent. The assumption that the non-adsorbed adenine surface concentration is small is difficult to prove, but is necessary so that a negligible contribution to I_p is made by diffusing species. Since the D.M.E. electrode area continuously increases with time, the amount of adenine adsorbed will increase with time and a concentration gradient will be present ; however, the cyclic voltammetric scans were made 12 s after the birth of a drop with a natural t_1 of ca. 14 s, so that the electrode area is not changing appreciably with time. For this reason, the concentration gradient is probably breaking down, and the assumption on which the calculation of an adsorbed state pK_a is based, is tenuous at best.

Conclusions

The adsorption of adenine from solutions of pH 4.8 is quite complex, *e.g.*, it may involve relatively slow kinetics due to the equilibrium between protonated and unprotonated adenine in solution near the solution| electrode interface as well as possibly a similar equilibrium involving adsorbed protonated and unprotonated adenine.

The use of the faradaic reduction of adenine as an index to the amount of adsorbed adenine present may be limited by the presence of a current component due to catalytic hydrogen discharge.

Acknowledgements

The authors thank the National Science Foundation, which helped support the work described. M. A. JENSEN thanks the ALLIED CHEMICAL & DYE CORPORATION for a fellowship.

References

1 V. VETTERL, *Collect. Czech. Chem. Commun.* **31,** 2105 (1966)
2 B. JANIK and P.J. ELVING, *J. Am. Chem. Soc.* **92,** 235 (1970)
3 J.W. WEBB, B. JANIK and P.J. ELVING, *J. Am. Chem. Soc.* **95,** 991 (1973)
4 J.W. WEBB, B. JANIK and P.J. ELVING, *J. Am. Chem. Soc.* **95,** 8495 (1973)
5 V. BRABEC and E. PALEČEK, *Stud. Biophys.* **60,** 105 (1976)
6 H. BERG, in *Topics in Bioelectrochemistry and Bioenergetics*, G. MILAZZO (Editor), John Wiley, London (1977) vol. **1,** p. 41
7 M.W. HUMPHREYS and R. PARSONS, *J. Electroanal. Chem. Interfacial Electrochem.* **75,** 427 (1977)
8 B. MALFOY, J.E. SEQUARIS, P. VALENTA and H.W. NÜRNBERG, *J. Electroanal. Chem. Interfacial Electrochem.* **75,** 455 (1977)
9 E. PALEČEK, V. BRABEC, F. JELEN and Z. PECHAN, *J. Electroanal. Chem. Interfacial Electrochem.* **75,** 471 (1977)
10 D. KRZNARIC, P. VALENTA and H.W. NÜRNBERG, *J. Electroanal. Chem. Interfacial Electrochem.* **65,** 863 (1975)
11 J. FLEMMING, *J. Electroanal. Chem. Interfacial Electrochem.* **75,** 421 (1977)
12 P.J. ELVING, J.T. MARKOWITZ and I. ROSENTHAL, *Anal. Chem.* **28,** 1179 (1956)
13 J.W. PERRAM, J.B. HAYTER and R.J. HUNTER, *J. Electroanal. Chem. Interfacial Electrochem.* **42,** 291 (1973)
14 D.M. MOHILNER, J.C. KREUSER, H. NAKADOMARI and P.R. MOHILNER, *J. Electrochem. Soc.* **123,** 359 (1976)
15 T.E. CUMMINGS, M. KATZ and P.J. ELVING, in preparation
16 M. VON STACKELBERG and H. FASSBENDER, *Z. Elektrochem.* **62,** 834 (1958)
17 D.L. SMITH and P.J. ELVING, *J. Am. Chem. Soc.* **84,** 1412 (1962)